PROCEEDINGS OF SCIENCE

Measurements of cosmic-ray anisotropies using LHAASO-WCDA

Wei Liu,[a,*] **Dong-xu Sun,**[b,d] **Dan Li,**[a,c] **Hong-bo Hu,**[a,c] **Qiang Yuan**[b,d] **and Yi-Qing Guo**[a,c] **on behalf of the LHAASO collaboration**

[a] *Key Laboratory of Particle Astrophysics, Institute of High Energy Physics, Chinese Academy of Sciences, Beijing 100049, China*

[b] *Key Laboratory of Dark Matter and Space Astronomy, Purple Mountain Observatory, Chinese Academy of Sciences, Nanjing 210023, China*

[c] *University of Chinese Academy of Sciences, Beijing 100049, China*

[d] *School of Astronomy and Space Science, University of Science and Technology of China, Hefei 230026, China*

E-mail: liuwei@ihep.ac.cn, sundx@pmo.ac.cn, lidan@ihep.ac.cn

The theoretical investigations have affirmed that the cosmic-ray (CR) anisotropy could help unveil the cosmic-ray origin, propagation and the local interstellar environment. Their precise measurements have been paid more and more attention in the recent years. As one of three principal facilities of the Large High Altitude Air Shower Observatory (LHAASO), the water Cherenkov detector array (WCDA) is composed of three water ponds and covers a total detection area of 87000 m^2. This makes it an ideal candidate for measuring the CR anisotropy from sub-TeV to ~ PeV. Since March 2021, WCDA has been in full operation with three ponds. In this contribution, we present the preliminary measurements of the CR anisotropy from ~ 1 TeV to ~ 150 TeV using two years of data, which contains ~ 230 billion events. The check of the analysis method have been done in anti-sidereal and extended-sidereal time frames, and the fluctuations in both frames are found to be small. The Compton-Getting effect in the solar time have been detected in the different energy bins. In terms of the above checks, the energy dependence of the CR anisotropy in the sidereal time are measured.

38th International Cosmic Ray Conference (ICRC2023)
26 July - 3 August, 2023
Nagoya, Japan

*Speaker

PoS(ICRC2023)186

1. Introduction

The abundant ground-based observations have revealed that the distribution of the Galactic CRs is not even, with the relative intensity varying from $\sim 10^{-4}$ to $\sim 10^{-3}$ to the average. It is called anisotropy. In the past years, more and more studies indicated that the CR anisotropy could unveil their acceleration sites, local propagation process and even the local magnetic environment.

However, the current measurements by the different experiments still have large uncertainties from several TeV to $\sim$ 1 PeV, due to the field of view, analysis method, energy calibration and other causes. Especially, the transition at $\sim$ 100 TeV are controversial. Above 100 TeV, the ASγ and ICECUBE experiment demonstrate the dipole phase turns to point the Galactic center [1–3], whereas the KASCADE experiment hints that the excess occurs in the direction of anti local regular magnetic field [4]. The precise measurement could determine the evolution of local diffusion with energy. In addition, recently Qiao et al. [5] expects that another dipole-phase reversal would occur at $\sim$ 200 GeV if the local source scenario is correct. The measurements of anisotropy at this energy could be an examination of the local source model.

The Large High Altitude Air Shower Observatory (LHAASO) is a hybrid extensive air shower observatory, which consists of three major arrays, i.e. square kilometer array (KM2A), water Cherenkov detector array (WCDA) and wide field-of-view air Cherenkov telescopes (WFCTA) [6]. It is located at Mt. Haizi (29°21′27.56″ N, 100°08′19.66″ E), at an altitude of 4410 m above the sea level, in Daocheng, Sichuan province of China. Compared with other available ground-based detectors in the similar energy range, LHAASO could observe a large portion of the sky with a higher recorded event rate. It could detect the CRs and γ-rays with energy from sub-TeV to $\sim$ 1000 PeV.

In this proceeding, we report on the preliminary analysis of the large-scale sidereal anisotropy of Galactic CRs using the two-years' WCDA data. The energy range extends from from $\sim$ 1 TeV to $\sim$ 150 TeV. The check of the analysis method have been done in anti-sidereal and extended-sidereal time frames, and the fluctuations in both frames are found to be small. The Compton-Getting effect in the solar time have been detected in the different energy bins. In terms of the above checks, the energy dependence of the CR anisotropy in the sidereal time are measured.

2. Detector and data set

The WCDA is located at the center of LHAASO, which consists of 3 water ponds with total area of $78,000$ m^2. Each of the two smaller ponds has an effective area of 150 m $\times$150 m, and the third has an area of 300 m $\times$110 m. Every pond is divided into 5 m $\times$5 m cells, which are separated by black plastic curtains. The first pond (called WCDA-1) is equipped with 900 pairs of 8-inch and 1.5-inch photomultiplier tubes (PMTs), the second (called WCDA-2) with 900 pairs of 20-inch and 3-inch PMTs, and the third (called WCDA-3) with 1320 pairs of same PMTs as WCDA-2. The PMTs reside at the bottom of the ponds, facing upward, to collect the Cherenkov lights generated by charged particles in the water. Fig 1 shows the layout of LHAASO-WCDA. For a more complete description of the WCDA, the calibration and the reconstruction procedure, one can refer to [7].

In this analysis, we present the preliminary results of the anisotropies in the TeV energies, using two years' data collected by the WCDA from April 1st 2021 to March 31th 2023. The CR events

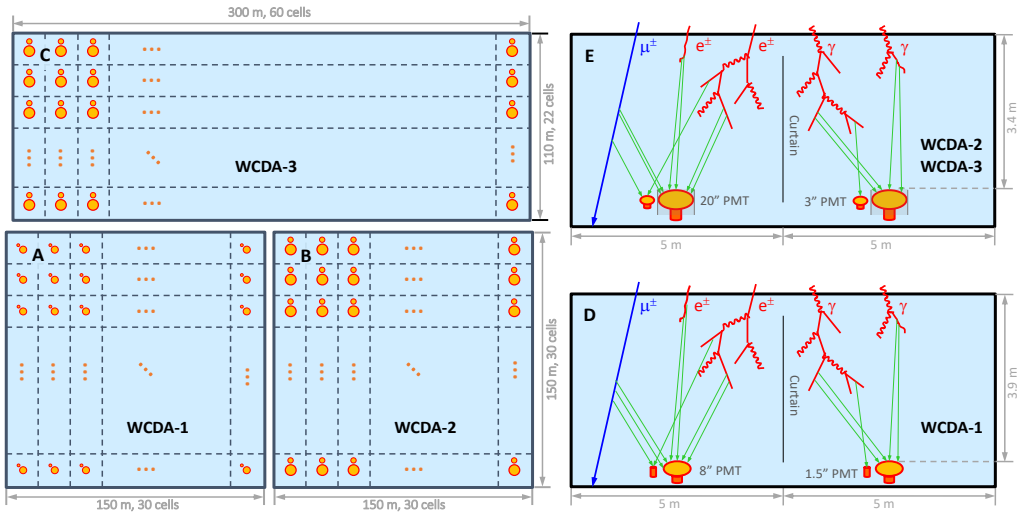

Figure 1: Layout of LHAASO-WCDA. (A–C) the detector layout for the thre ponds, with black dashed lines representing the plastic curtains partitioning the array into cells. Two sets of circles representing the big (8-inch for WCDA-1, 20-inch for WCDA-2 and WCDA-3) and small (1.5-inch for WCDA-1, 3-inch for WCDA-2 and WCDA-3) PMTs. (E–D) show side views of two cells, as well as schematic physics processes (red wavy line: Gamma; red straight line: electron or positron; blue line: muon; green line: Cherenkov light). The water depth over the PMT top surface is 3.9 m for WCDA-1 and 3.4 m for WCDA-2 3.

are selected based on the following criteria: 1) estimated air shower core location should be within 120 metres from the WCDA center; 2) the zenith angle of the incident direction should be less than 50°, which corresponds to the observed region in the declination band from −20° to 80°; 3) $N_{\rm hit}$ is selected as the shower energy estimator. It is defined as the equivalent number of fired cells with a specific normalized charge threshold in a time window of ±30 ns surrounding the reconstructed shower front. In this report, $N_{\rm hit}$ of the three pools should be large than 60, which corresponds to the reconstructed energy large than 1 TeV. After selection, about 2.3×10^{11} CR events are used in the present analysis.

To measure the energy dependence of anisotropies, the data are divided into 8 intervals based on $N_{\rm hit}$. The correlation between the primary energy and $N_{\rm hit}$ is established by the Monte Carlo simulations using Corsika and Geant4. Figure 2 plots the primary energy distributions for CR showers for the 8 $N_{\rm hit}$ bins. The median energy of the distributions are used as the measure of the CR primary energy in the corresponding $N_{\rm hit}$ bin. Table 1 lists the median energies and corresponding number of CR events for different $N_{\rm hit}$ bins.

3. Analysis method

As far as we know, the observed anisotropies have two origins. One is the anisotropy in the sidereal time frame, which arises from the uneven distribution of CR sources and CR propagation in the Galaxy. There is another origin of anisotropy in the sidereal time, which stems from the motion of the solar system around Galaxy. It is named as the Compton-Getting (CG) effect, which is essentially a kinematic effect. However the different experiments did not detect this effect. The other is also a kind of kinematic effect and observed in the solar time frame. It originates from the

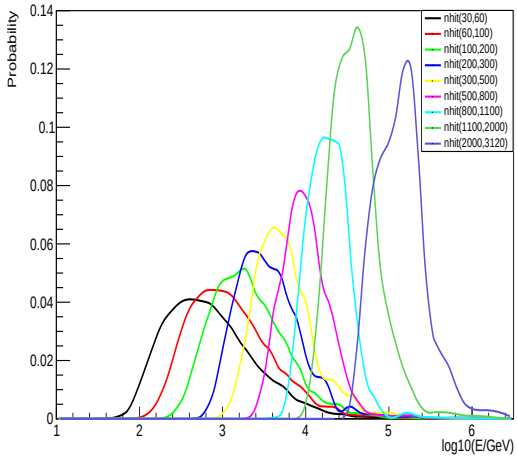

Figure 2: Normalized distributions of primary energy of CR showers.

Table 1: $N_{\rm hit}$ range, median energy $E_{\rm med}$ and number of CRs in the different $N_{\rm hit}$ intervals.

$N_{\rm hit}$	$E_{\rm med}$/TeV	number of CRs
60-100	1.1	1.11025e+11
100-200	1.9	7.27811e+10
200-300	3.2	2.14185e+10
300-500	5.1	1.53454e+10
500-800	9.5	7.11632e+09
800-1100	18.4	2.44981e+09
1100-2000	37.6	1.78765e+09
2000-3120	136.0	2.89945e+08

revolution of the Earth around the solar system. It is also called the solar Compton-Getting (CG) effect. To measure the sidereal anisotropy accurately, one should remove the interference from the solar Compton-Getting (CG) effect. However, the diurnal and seasonal variations of atmospheric pressure and temperature, operation problem of the detectors etc. would change the collected event rate. These factors would produce the modulation between sidereal and solar anisotropies and hamper the measurement of the sidereal anisotropy. When the modulation , it also occurs in the other two hypothetical time frame, anti-sidereal and extended-sidereal respectively. To estimate the systematic errors of our measurements, we also have to examine the intensities of anisotropies in the anti-sidereal and extended-sidereal time frames.

The analysis method in this work is based on the so-called All Distance Equi-Zenith Angle method [8, 9]. In this method, the equi-zenith angle assumption is adopted. For a candidate "on-source window", the side band of the same zenith angle belt is used as the "off-source windows" to estimate the background events. This method could eliminate various detection effects caused by the instrumental and environmental variations, such as changes in pressure and temperature, which are hard to be controlled and tend to introduce systematic errors in measurement.

In this work, an improved method is applied by simultaneously fitting the modulation in all four different time frames, i.e. sidereal, solar, anti-sidereal and extended-sidereal respectively [10]. At any moment t, the relative intensity of CRs at any given direction (θ, ϕ) in the horizontal coordinate, is a product of $I_{\rm sid}(\alpha_{\rm sid}, \delta_{\rm sid})$, $I_{\rm sol}(\alpha_{\rm sol}, \delta_{\rm sol})$, $I_{\rm asid}(\alpha_{\rm asid}, \delta_{\rm asid})$ and $I_{\rm esid}(\alpha_{\rm esid}, \delta_{\rm esid})$. I_{sid}, I_{sol}, I_{asid} and I_{esid} denote the intensity of CR anisotropy in the sidereal, solar, anti-sidereal and extended-sidereal time frames respectively. And $(\alpha_{\rm sid}, \delta_{\rm sid})$, $(\alpha_{\rm sol}, \delta_{\rm sol})$, $(\alpha_{\rm asid}, \delta_{\rm asid})$ and $(\alpha_{\rm esid}, \delta_{\rm esid})$ correspond to the celestial coordinate for the four time frames respectively for the same point (θ, ϕ) at moment t. So the total χ^2 can be written as

$$\chi^2 = \sum_{t,\theta,\phi} \left(\left\{ \frac{N_{\rm obs}(t,\theta,\phi)}{I(\alpha,\delta)} - \frac{\sum\limits_{\phi\neq\phi'} [N_{\rm obs}(t,\theta,\phi')/I(\alpha,\delta)]}{\sum\limits_{\phi\neq\phi'} 1} \right\}^2 \times \left\{ \frac{N_{\rm obs}(t,\theta,\phi)}{I^2(\alpha,\delta)} + \frac{\sum\limits_{\phi\neq\phi'} [N_{\rm obs}(t,\theta,\phi')/I(\alpha,\delta)]}{(\sum\limits_{\phi\neq\phi'} 1)^2} \right\}^{-1} \right). \quad (1)$$

where $I(\alpha,\delta) = I_{\rm sid}(\alpha_{\rm sid}, \delta_{\rm sid}) \cdot I_{\rm sol}(\alpha_{\rm sol}, \delta_{\rm sol}) \cdot I_{\rm asid}(\alpha_{\rm asid}, \delta_{\rm asid}) \cdot I_{\rm esid}(\alpha_{\rm esid}, \delta_{\rm esid})$. $N_{\rm obs}(t,\theta,\phi)$ is the number of observed events in the "window" (θ, ϕ) at the moment t. After minimizing the χ^2 function, the four 2D skymaps, i.e. $I_{\rm sid}$, $I_{\rm sol}$, $I_{\rm asid}$ and $I_{\rm esid}$, can be obtained simultaneously. Lacking the absolute detector efficiency calibration in the declination direction, the absolute intensities of anisotropies along different Dec direction cannot be compared. Thus the average intensity in each narrow Dec belt is normalized to unity.

4. Measurements of the anisotropies

To evaluate the mutual inference between sidereal and solar anisotropies and estimate the systematic errors in this measurement, the anti-sidereal and extended-sidereal anisotropies are calculated respectively. In the anti-sidereal time frame, there is no significant excesses or deficits with significance over 5 sigma at lower energies. But the intensity maps of extended-sidereal anisotropy show some structures at lower energies, although not larg. It may be affected by the running status of the detectors. We are now performing the data check further. At the high energy, the amplitude of structures becomes large compared to the lower energy, which may attributed to the less event number.

For the solar CG effect, it is predicted to taken on a dipole oscillation with phase. Furthermore, the amplitude is expected to be about 4×10^{-4} and does not vary with energy. And the phase always point toward 6 hrs. Therefore the solar CG effect can be used to verify the analysis method. Figure 3 shows the 2D intensity maps of the solar anisotropy for different energies. The dipole structures can be clearly seen in the various energies, except the last bin due to the inadequate data at high energy.

Figure 4 shows the 1D projection along the R.A. direction for the 2D maps. The 1D distributions are fitted using first harmonic to obtain the energy dependence of the amplitude and the phase. Except the last two bins, both amplitude and phase are consistent with the expectation, namely amplitude $\sim 4\times10^{-4}$, phase at 6 hrs. In the last energy bin, the CG effect is invisible, due to the inadequate data. The data shows principally fluctuations. For the penultimate bin, the amplitude

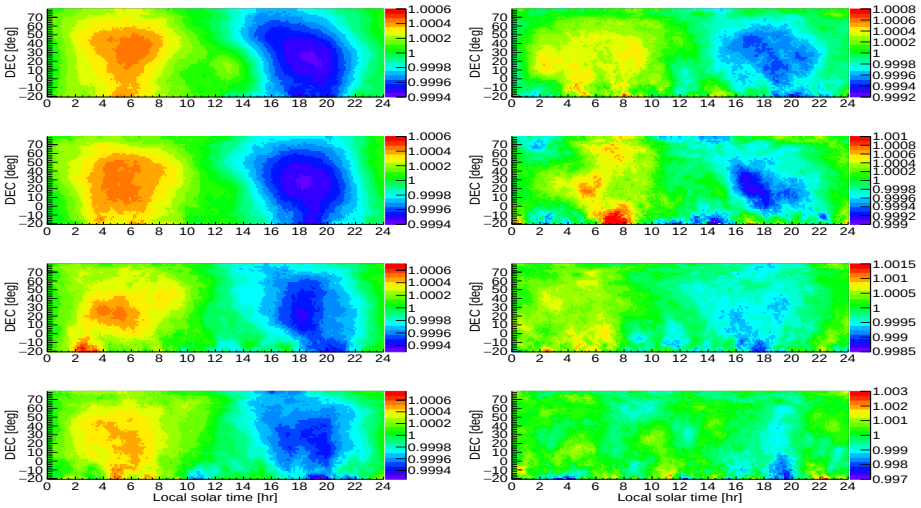

Figure 3: 2D intensity maps of the anisotropy in the solar time frame for different energies.

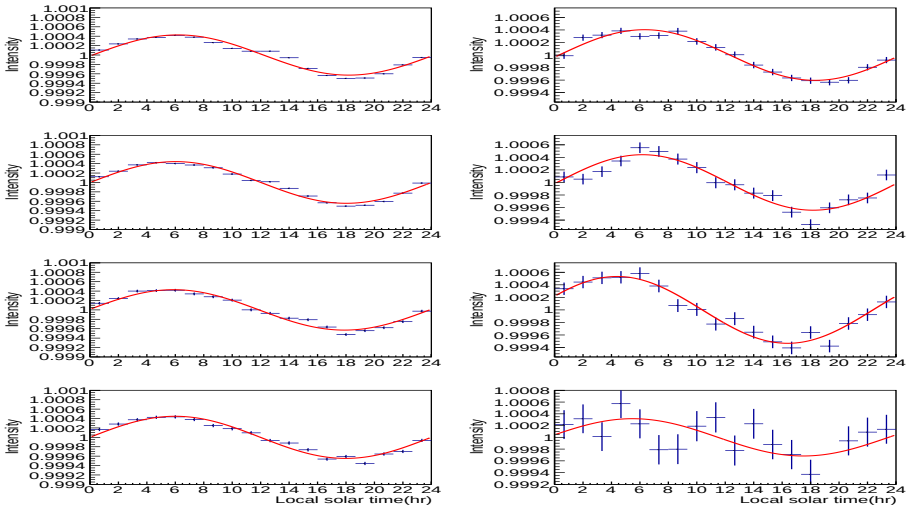

Figure 4: 1D projection of the 2D solar anisotropies in R.A. direction.

and phase seems to deviate from the expectation. It may originate from the interference of the sidereal anisotropy due to the non-uniform data. We are now further check data to remove the interference. But we want to stress that at tens of TeV, the amplitude of dipole anisotropy is larger enough, and the interference of solar anisotropy on the sidereal anisotropy is negligible.

Figure 5 illustrates the energy dependence of the sidereal anisotropy in the 2D maps. The left column is the relative intensities of the anisotropy at different energies, and the right column corresponds to the significance. The The energy spans from ~ 1 TeV to ~ 140 TeV. Below ~ 30 TeV, the anisotropies do not show significant variation with energy. But above ~ 30 TeV, the previous anisotropies start to fade away. This is consistent with other observations.

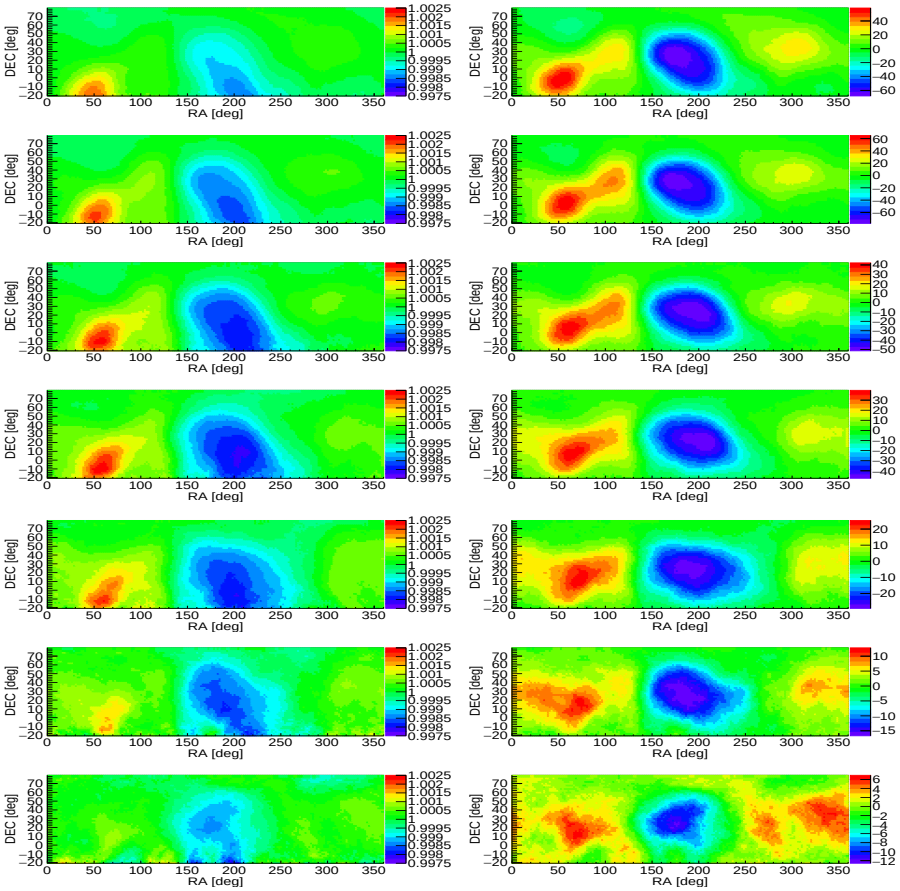

Figure 5: 2D maps of the sidereal anisotropies at different energies.

5. Discussion

The LHAASO-WCDA has been in full operation over two years. In this talk, we report the measurements of the large-scale sidereal anisotropy using the data with two-year period. We check solar CG effect at different energties, which are consistent with the expectation. The sidereal anisotropy are detected and their energy dependence is consistent with the other experiments, e.g. ASγ, ARGO-YBJ, and HAWC. We are now further checking the possible cross-talk between sidereal and solar anisotropies.

References

[1] M. G. Aartsen, K. Abraham, M. Ackermann, et al. Anisotropy in Cosmic-Ray Arrival Directions in the Southern Hemisphere Based on Six Years of Data from the IceCube Detector. , 826(2):220, August 2016.

[2] M. Amenomori, X. J. Bi, D. Chen, et al. Northern Sky Galactic Cosmic Ray Anisotropy between 10 and 1000 TeV with the Tibet Air Shower Array. , 836(2):153, February 2017.

[3] B. Bartoli, P. Bernardini, X. J. Bi, et al. Galactic Cosmic-Ray Anisotropy in the Northern Hemisphere from the ARGO-YBJ Experiment during 2008-2012. , 861(2):93, July 2018.

[4] A. Chiavassa, W. D. Apel, J. C. Arteaga-Velázquez, et al. A study of the first harmonic of the large scale anisotropies with the KASCADE-Grande experiment. In *34th International Cosmic Ray Conference (ICRC2015)*, volume 34 of *International Cosmic Ray Conference*, page 281, July 2015.

[5] Bing-Qiang Qiao, Qing Luo, Qiang Yuan, and Yi-Qing Guo. Understanding the Phase Reversals of Galactic Cosmic-Ray Anisotropies. , 942(1):13, January 2023.

[6] Andrea Addazi et al. The Large High Altitude Air Shower Observatory (LHAASO) Science Book (2021 Edition). *Chin. Phys. C*, 46:035001–035007, 2022.

[7] F. Aharonian, Q. An, Axikegu, et al. Performance of lhaaso-wcda and observation of the crab nebula as a standard candle *. *Chinese Physics C*, 45(8):085002, aug 2021.

[8] M. Amenomori, S. Ayabe, D. Chen, et al. A Northern Sky Survey for Steady Tera-Electron Volt Gamma-Ray Point Sources Using the Tibet Air Shower Array. , 633(2):1005–1012, November 2005.

[9] M. Amenomori, S. Ayabe, X. J. Bi, et al. Anisotropy and Corotation of Galactic Cosmic Rays. *Science*, 314(5798):439–443, October 2006.

[10] M. Amenomori, X. J. Bi, D. Chen, et al. On Temporal Variations of the Multi-TeV Cosmic Ray Anisotropy Using the Tibet III Air Shower Array. , 711(1):119–124, March 2010.